

# ANALYSIS OF NOZZLE LOADS FOR PROCESS PUMPS

by

**Takio Shimizu**

Senior Research Engineer

Ebara Research Company, Limited

and

**Hironori Teshiba**

Senior Engineer

Ebara Corporation

Tokyo, Japan



*Takio Shimizu is a Senior Research Engineer in charge of strength analysis with Ebara Research Company, Fujisawa, Japan.*

*Mr. Shimizu is a stress analysis specialist. During the past 12 years, he has been involved in strength evaluation projects for pumps, blowers and associated components.*

*Presently, he is engaged in a stress and strength analysis program for computed aided design of pumps and blowers.*

*He graduated from Tokyo Metropolitan University with a B.S. degree in mathematics.*

---



*Hironori Teshiba is a Senior Engineer responsible for pump planning and application in Ebara Corporation's Tokyo Office.*

*Since joining Ebara Corporation, he has held several centrifugal pump design and development positions.*

*He holds an M.S. degree in Mechanical Engineering from Chuoh University in Japan.*

---

## ABSTRACT

Under extreme conditions, pumps may be required to withstand severe nozzle loads, which often exceed the API 610 specified values. To meet these requirements, pump mechanical behavior versus nozzle loads must be examined in detail.

Others have discussed shaft end displacement of centerline mounted pumps under nozzle loads. However, the subject of stresses on the pedestal bolts and casing is a critical area that must also be analyzed.

An in-depth study was made on the deformation and stress analysis of centerline mounted end suction pumps, whose stiffnesses were relatively low and were frequently required to withstand rather high nozzle loads. The nozzle load analysis consisted of deformation and stress measurements, combined with finite element calculation.

The analysis resulted in a versatile empirical formula for end suction, centerline mounted pumps that can be used to estimate the shaft end displacement, pedestal bolt stress and casing stress for arbitrary nozzle loads. This allows the determination of

whether or not specified nozzle loading conditions can be tolerated by a given pump and pump support design.

## INTRODUCTION

Pumps are affected by the static and thermodynamic loads which are imposed from their piping systems. If these loads exceed the pump manufacturer's allowable limits, mechanical damage may occur, due to shaft displacement and/or overstressed components.

API 610 (Sixth Edition) has specified nozzle loading criteria for process pumps with flange sizes from two through sixteen inches [1]. In addition, this specification requires that the pumps be able to withstand twice these forces and moments when applied simultaneously. The API 610 specification establishes criteria for both the pump manufacturer and the piping system design engineer; however, these nozzle loads are often exceeded in actual practice due to improper system analysis, abnormal process conditions, space limitations, foundation settling, etc.

In a realistic sense, the pump manufacturer must be able to analyze and understand the effects of nozzle loading on a pump's mechanical behavior. In general, theoretical analysis of nozzle loads versus pump behavior is difficult, because of complicated casing shapes and a wide variety of designs. Therefore, only a few investigative reports have been published on this subject [2, 3, 4].

An in-depth research project which evaluates shaft displacement, casing stress, bolting stress and baseplate design for various nozzle loads is addressed herein. The evaluation was conducted for API 610 end suction, process pumps and compares the results from actual test measurements to theoretical calculations.

As a final result, empirical relations were derived which enable accurate calculations of shaft end displacement, pedestal bolt stress and casing stress for arbitrary nozzle loads. These calculation methods only apply to centerline mounted, end suction pump designs.

## PUMP STRUCTURAL DESIGN AND DESIGN RELATIONSHIPS

A sectional view of a centerline mounted, end suction pump is shown in Figure 1. This view identifies the location of major components. A complete pump package with baseplate, motor driver, etc., is shown in Figure 2. Also, a typical baseplate designed to minimize deflection caused by excess nozzle loading and meet other API 610 (Sixth Edition) criteria is illustrated in Figure 3.

In the past, a simple correlation between shaft displacement and pump nozzle dimensions has not been derived because it is

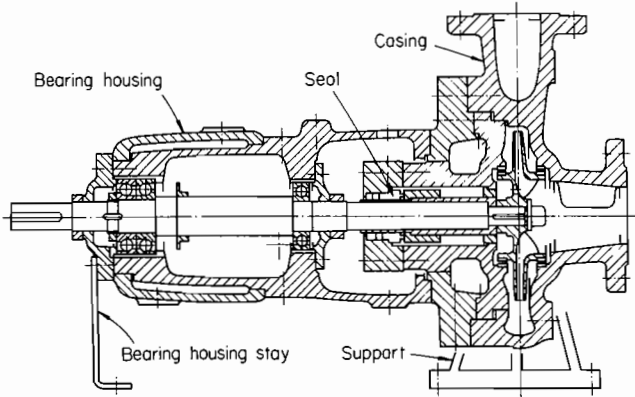


Figure 1. Sectional View of Centerline Mounted, End Suction Pump.

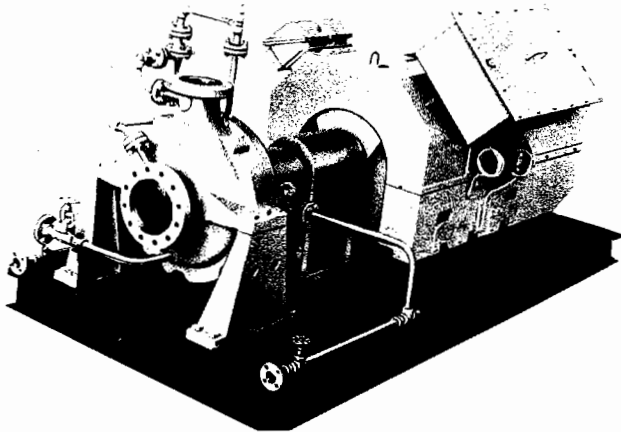


Figure 2. Complete Pump Package.

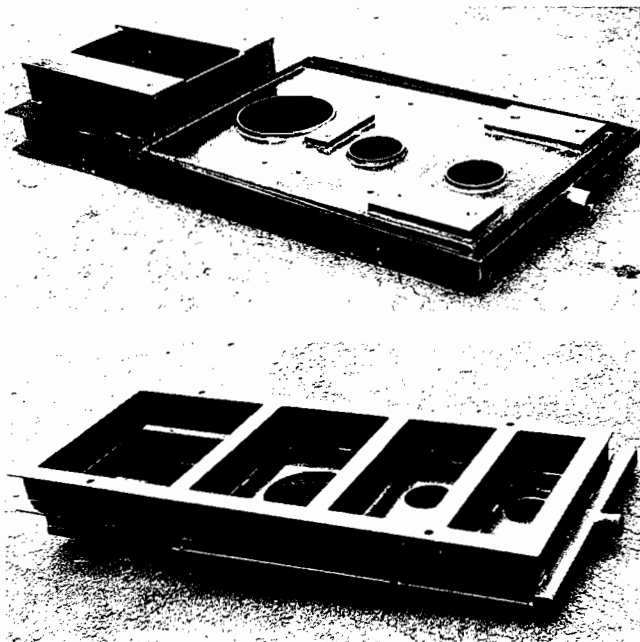


Figure 3. Views of Pump Baseplate.

dependent on the pump support design (pedestals, bearing housing stay and baseplate). Shaft end displacement must be determined in each case by considering support component stiffnesses in conjunction with an overall analysis of the nozzle forces and moments. This is a difficult task because of the complex relationship between the pump and pump support components. The only realistic method of gaining accurate data was to set up an actual testing program to obtain stress and deflection results from known nozzle forces and moments. The test data would then be analyzed to develop an empirical relationship, if possible, and compared to other theoretical calculation methods.

The pump model line which was analyzed included 40 pumps with flange sizes varying from two through twelve inches.

An empirical relationship was developed between the pump casing stress and the pump nozzle dimensions. Also, the test results were similar to those calculated by finite element analysis.

### NOZZLE LOAD TESTING PROGRAM

In order to determine whether or not various nozzle loadings would produce acceptable results, the following must be measured:

- Shaft End Displacement
- Casing Stress
- Bolting Stress

The acceptable shaft end displacement criteria was based on API 610 (Sixth Edition) limitations: 0.005 in in any direction when subjected to twice the published forces and moments. The nozzle loading would be analyzed on an individual load basis and during the simultaneous application of several loads.

The casing and bolt stress would be limited to ensure that reasonable design safety factors would be maintained. These will be examined in detail in other sections.

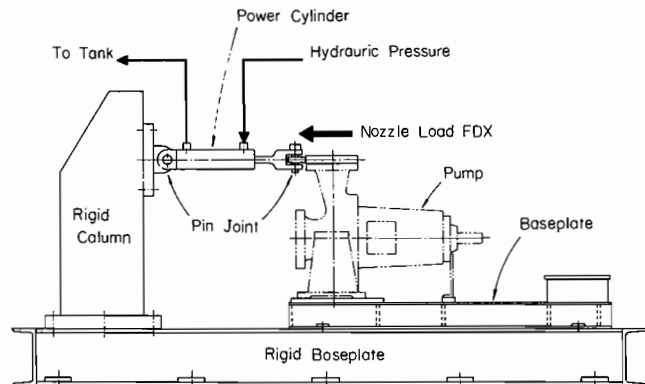
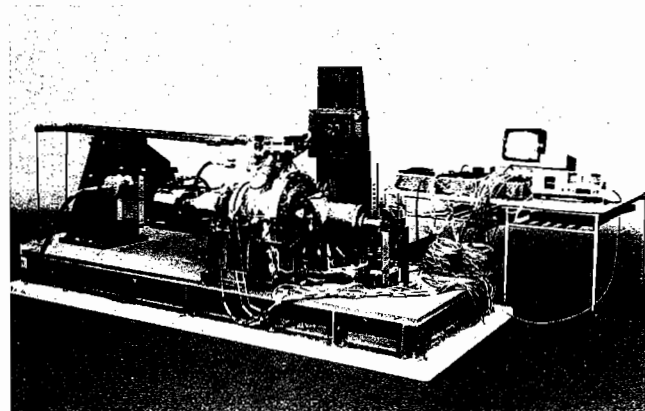


Figure 4. Experimental Test Stand.

### Test Apparatus and Procedures

A unique nozzle load testing device was designed and manufactured specifically for testing purposes, as shown in Figure 4. Loads on both suction and discharge nozzles can be independently generated and simultaneously applied. This is accomplished via a power cylinder, with a rotary ram and a universal joint connected to each flange. Not only does this method allow application of a pure force and/or moment, it also allows extremely accurate measurement of these values.

Three axis strain gauges were used to measure casing and bolting strains (and calculated stresses) at 34 different locations. Also, strain gauge type displacement meters were used to measure deflections at 24 additional locations, including shaft end, bearing housing, pedestals and baseplate.

Three representative pump sizes were analyzed with flange sizes of  $3 \times 2$ ,  $6 \times 4$  and  $8 \times 6$ . If correlation factors did not show distinctive profiles, additional pump sizes could have to be tested; however, data from these pump sizes was sufficient.

These pumps were tested in two modes. The first included a bare pump with centerline support pedestals only, as shown in Figure 5, and the second included a bare pump with mounting pedestals bolted to a baseplate and coupled to a motor driver (not operated).

Twelve types of nozzle forces and moments were applied as illustrated in Figure 5. The loads were brought up to API 610 (Sixth Edition, Table 2) values and then increased by whole number multipliers until the shaft end displacement equaled or exceeded five mils (0.005 in). Various forces and moments were also applied in several types of simultaneous combinations.

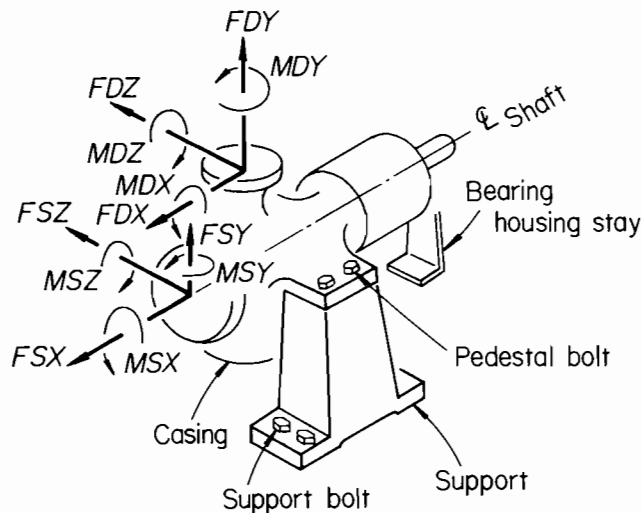


Figure 5. Definition of Nozzle Loads.

## NOZZLE LOAD TESTING RESULTS

### Casing Stress

All of the casing stress testing was done on pumps mounted on pedestals and bearing housing stays which were bolted to the rigid test bed (i.e., no baseplate).

The larger casing stresses occurred at the suction and discharge nozzles. The maximum casing stress occurred in the suction nozzle when the bending moment MSY was applied. This is illustrated by the stress point measurements and locations in Table 1.

Table 1. Shaft End Displacements and Maximum Casing Stresses. ( $8 \times 6 - 10$ ).

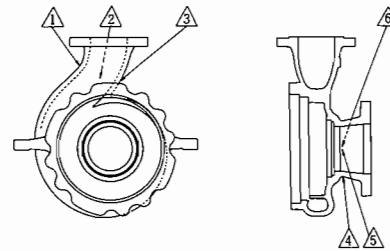
Nozzle load (lb or ft-lb)	Shaft end displacement		Maximum casing stress		
	Uy (Mils)	Uz (Mils)	Place	Direction	Stress (ksi)
FSX 1100	0.22	0.	6	$\sigma_\varphi$	0.33
FSY 700	-0.72	-0.12	4	$\sigma_\varphi$	0.17
FSZ 850	-0.01	1.63	6	$\sigma_\varphi$	0.40
FDX 560	1.43	0.20	2	$\sigma_\varphi$	0.20
FDY 700	-0.01	0.03	3	$\sigma_\varphi$	0.04
FDZ 460	-0.01	1.10	1	$\sigma_\varphi$	0.13
MSX 2600	0.35	0.38	6	$\sigma_{\theta\varphi}$	0.87
MSY 1900	0.43	1.38	5	$\sigma_\varphi$	2.74
MSZ 1300	-1.19	-0.21	4	$\sigma_\varphi$	0.55
MDX 1700	-0.20	0.39	1	$\sigma_\varphi$	1.17
MDY 1300	-0.01	1.06	3	$\sigma_{\theta\varphi}$	0.41
MDZ 870	-1.11	0.33	1	$\sigma_\varphi$	0.34

Direction of stress

$\sigma_\varphi$ : Stream line direction

$\sigma_{\theta\varphi}$ : Direction inclining at 45 deg. to streamline

Places where maximum stresses generate



In addition, the maximum casing stress versus API 610 load ratio is shown in Figure 6. The load ratio was calculated in the following manner:

$$\text{API 610 Load Ratio} = F(*)/F(*, \text{API})$$

where

\* = Type of nozzle load

F(\*) = Applied Test Load

F(\*, API) = API 610 (6th Ed.) Allowable loads in API 610 Table 2.

This also indicates that the bending moment MSY is the most significant.

### Bolt Stress

The centerline support pedestal bolting to the baseplate is normally stronger than the pump-to-pedestal bolting, because there are more bolts and large bolts holding the pedestal to the baseplate. This is also true for pedestals which are welded to the baseplate support structure. Therefore, the critical area of bolting stress analysis is concerned with the bolts that hold the pump to the pedestal. All of the bolt stress testing was done on pumps without baseplates.

"Nominal stress" of a bolt is defined as the force applied to the bolt divided by the effective sectional area of the bolt. The additional bolt stress above the initial tightening stress is not significantly increased by nozzle loading until the "nominal

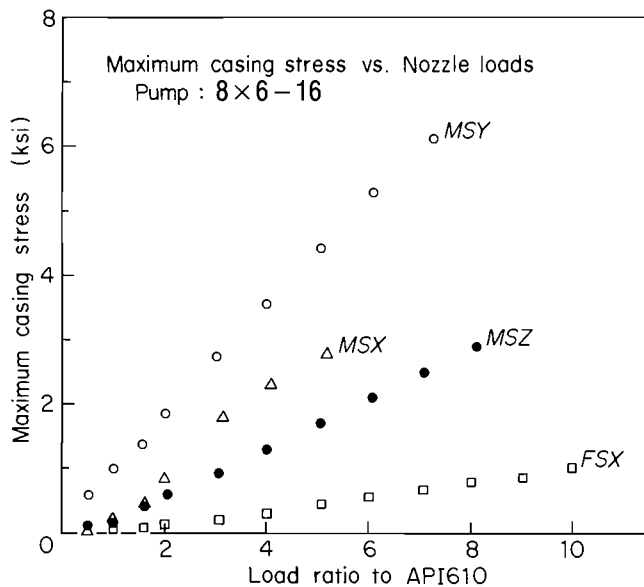


Figure 6. Casing Stress of Pump Due to Applied Nozzle Loads.

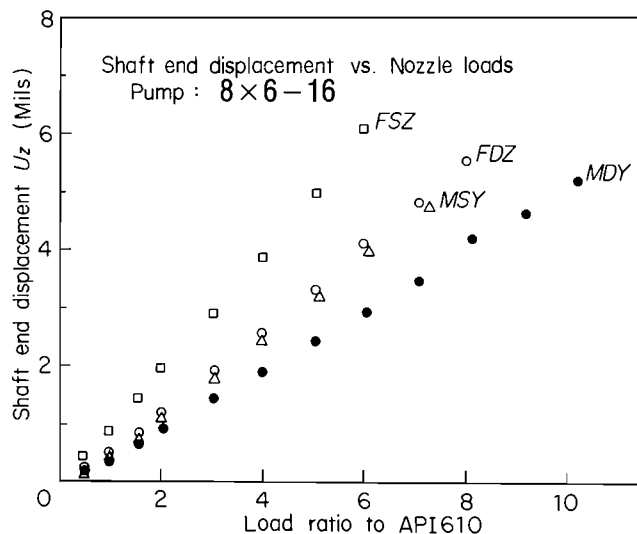


Figure 8. Shaft End Displacement of Pump Due to Applied Nozzle Loads.

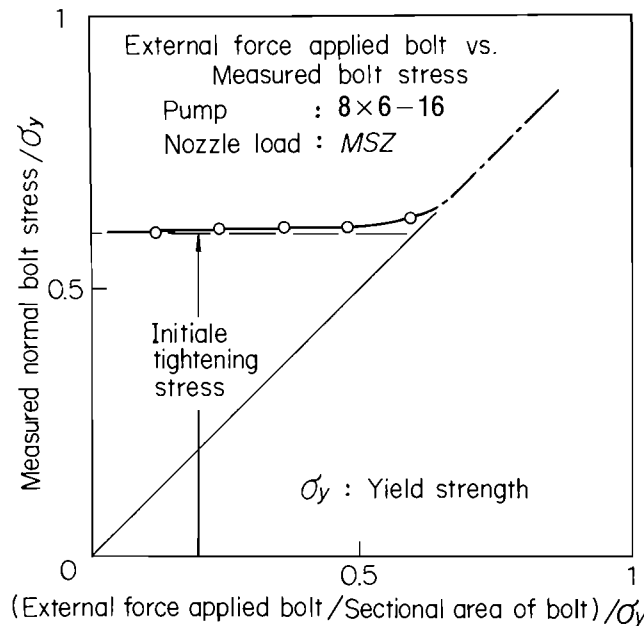


Figure 7. Pedestal Bolt Stress of Pump Due to Applied Nozzle Load.

stress" equals approximately 60 percent of the material yield strength. This is illustrated in Figure 7.

On all of the tested pumps, the "nominal stress" of the pump-to-pedestal bolting was less than 60 percent of the yield strength when API 610 (Sixth Edition) loads were applied in all arbitrary combinations.

This bolt stress criteria is suitable for API 610 (Sixth Edition) loads and it is recommended for bolt design.

**Shaft End Displacement**

The following are relative trends in shaft displacement versus application of individual forces and moments:

- FSY, MSZ, FDX, MDZ → Y Direction Displacement
- FSZ, MSY, FDZ, MDY → Z Direction Displacement
- FSZ, MSX, FDY, MDX → Negligible Displacement

These can also be seen in Table 1. The Z direction displacement for an 8 x 6 pump is illustrated in Figure 8. Several combinations of two loads were applied and the shaft displacement under these conditions was approximately equal to the arithmetic sum of the shaft displacements with individual loads.

The effect of pump size on shaft deflections was also analyzed. Larger pump sizes have greater shaft end displacements which are caused by the lower rigidity of the pump (Figure 9).

Shaft displacement was also evaluated for bare pumps with pedestals only and pump packages including baseplate, motor, coupling, etc. As shown in Table 2, the baseplate mounted pumps exhibited 1.2 to 4.3 times the shaft displacement of the bare pump with pedestal only. The displacement occurring at various points along the 8x6 pump when FDX is applied is illustrated in Figure 10. The displacement of the shaft end (Point C) is approximately the same as the extended deformation of support. This indicates that the shaft displacement can be determined by the support stiffness. These results were similar for the other size pumps tested.

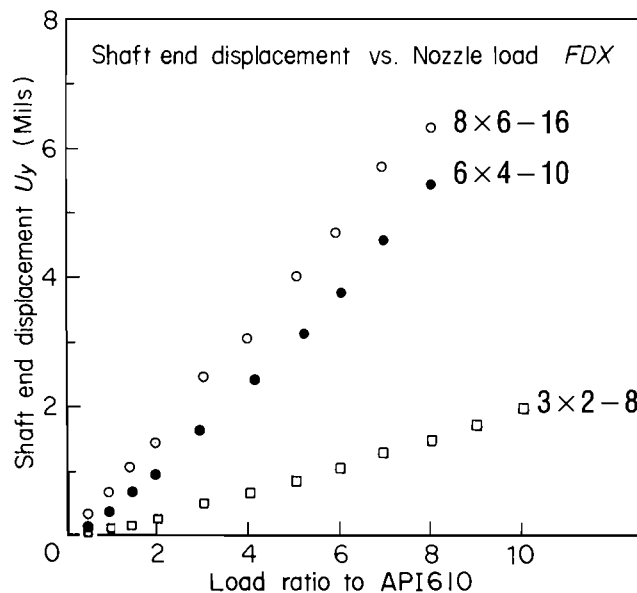


Figure 9. Influence of Pump Size on Shaft End Displacement.

Table 2. Relative Shaft End Displacements of Pump Installed on Base, and Shaft End Displacements of Pump without Base. (8x6-10).

Nozzle load (lb or ft-lb)	Relative displacement with base		Shaft end displacement without base	
	Direction	Displacement (Mils)	Direction	Displacement (Mils)
FSX 1100	y	0.97	y	0.22
FSY 700	y	-1.04	y	-0.72
FSZ 850	z	2.02	z	1.63
FDX 560	y	2.57	y	1.43
FDZ 460	z	1.34	z	1.10
MSZ 1300	y	-2.37	y	-1.19
MDZ 870	y	-1.86	y	-1.11

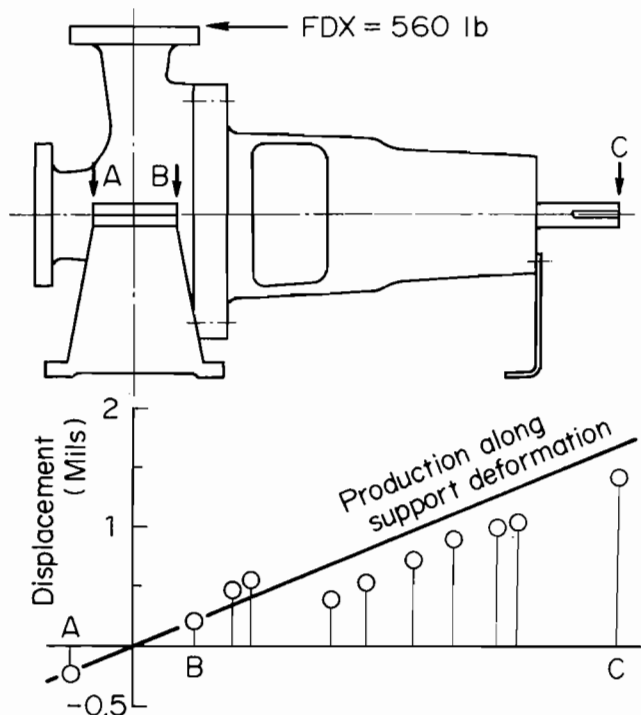


Figure 10. Displacement Distribution Along Z-Axis Due to Applied Nozzle Load. (8x6-10).

Internal Contact

Internal contact was checked via rotating the shaft by hand during load testing. No internal contact was detected for any of the pumps tested even when loads from five to ten times API 610 (Sixth Edition) load limits were applied to the nozzle.

THEORETICAL FINITE ELEMENT ANALYSIS

Method of Analysis

A finite element analysis (MSC/NASTRAN Program) was conducted on eight pumps and ten baseplate sizes. These pumps were the same type as previously tested and included the actual load tested pumps. It should also be noted that three of these

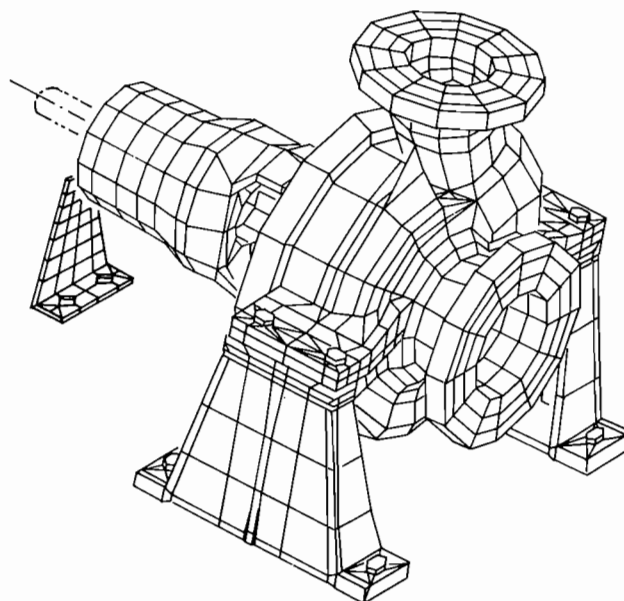


Figure 11. Mesh Pattern for Finite Element Analysis.

pumps had single volute casings and five pumps had double volute casings.

The mesh pattern for the finite element analysis is shown in Figure 11.

Table 3. Shaft End Displacements and Maximum Casing Stresses by Finite Element Analysis as Compared to Actual Load Test Values (Pump: 8x6-10).

Nozzle load (lb or ft-lb)	FEM analysis					Actual load test				
	Shaft end displacement		Maximum casing stress			Shaft end displacement		Maximum casing stress		
	Uy (Mils)	Uz (Mils)	Place	Direction	Stress (ksi)	Uy (Mils)	Uz (Mils)	Place	Direction	Stress (ksi)
FSX 1100	0.19	0.03	6	$\sigma_{\phi}$	0.30	0.22	0.	6	$\sigma_{\phi}$	0.33
FSY 700	-0.54	0.05	4	$\sigma_{\phi}$	0.17	-0.72	-0.12	4	$\sigma_{\phi}$	0.17
FSZ 850	0.01	1.29	6	$\sigma_{\phi}$	0.24	-0.01	1.63	6	$\sigma_{\phi}$	0.40
FDX 560	0.96	-0.07	2	$\sigma_{\phi}$	0.16	1.43	0.20	2	$\sigma_{\phi}$	0.20
FDY 700	0.	0.03	3	$\sigma_{\phi}$	0.01	-0.01	0.03	3	$\sigma_{\phi}$	0.04
FDZ 460	0.01	0.81	1	$\sigma_{\phi}$	0.14	-0.01	1.10	1	$\sigma_{\phi}$	0.13
MSX 2600	0.04	0.35	6	$\sigma_{\phi\phi}$	0.57	0.35	0.38	6	$\sigma_{\phi\phi}$	0.87
MSY 1900	-0.03	1.25	5	$\sigma_{\phi}$	1.52	0.43	1.38	5	$\sigma_{\phi}$	2.74
MSZ 1300	-1.35	-0.03	4	$\sigma_{\phi}$	0.90	-1.19	-0.21	4	$\sigma_{\phi}$	0.55
MDX 1700	0.01	0.26	1	$\sigma_{\phi}$	1.04	-0.20	0.39	1	$\sigma_{\phi}$	1.17
MDY 1300	0.01	0.91	3	$\sigma_{\phi\phi}$	0.81	-0.01	1.06	3	$\sigma_{\phi\phi}$	0.41
MDZ 870	-0.87	0.10	1	$\sigma_{\phi}$	0.43	-1.11	0.33	1	$\sigma_{\phi}$	0.34

Table 4. Measured and Analyzed Relative Shaft End Displacements (Pump: 8x6-10).

Nozzle load (lb or ft-lb)	ACTUAL TEST RESULT		FEM analysis	
	Direction	Displacement (Mils)	Direction	Displacement (Mils)
FSX 1100	y	0.97	y	0.93
FSY 700	y	-1.04	y	-0.85
FSZ 850	z	2.02	z	1.68
FDX 560	y	2.57	y	2.10
FDZ 460	z	1.34	z	1.05
MSZ 1300	y	-2.37	y	-2.53
MDZ 870	y	-1.86	y	-1.61

**Analysis Results**

The results of the 8 × 6 pump finite element analysis are shown in Table 3, which also indicates the nozzle load test results from Table 1. The analysis results and the actual test results are in general agreement. Therefore, the validity of the finite element analysis is confirmed for casing stress values.

Deformations of the baseplate as measured in actual test results and as calculated by finite element analysis (FEM) are also in close agreement. These results are compared in Figure 12.

Therefore, the relative shaft displacement can be accurately obtained by finite element analysis. The actual test results for the

8 × 6 pump and FEM analysis are similar, as shown in Table 4. The pump was baseplate mounted and coupled to a motor driver.

**FORMULAS FOR CALCULATING MAXIMUM CASING STRESS**

In order to relate casing stress to pump nozzle parameters, an empirical relationship was derived. This relation is based on the following:

$$\text{Casing Stress Coefficient} = \alpha = \frac{\sigma \text{ max.}}{M_{SY}/d_m^2 t}$$

where

$\sigma \text{ max.}$  = Maximum casing stress generated by  $M_{SY}$

$M_{SY}$  = Suction nozzle moment

$d_m$  = Mean diameter of suction nozzle

$t$  = Mean thickness of suction nozzle

Pump size parameter =  $D_e = D_o + D_d$

where

$D_o$  = Volute internal diameter

$D_d$  = Diameter of discharge nozzle

This relation is illustrated in Figure 13 for single and double volute pumps.

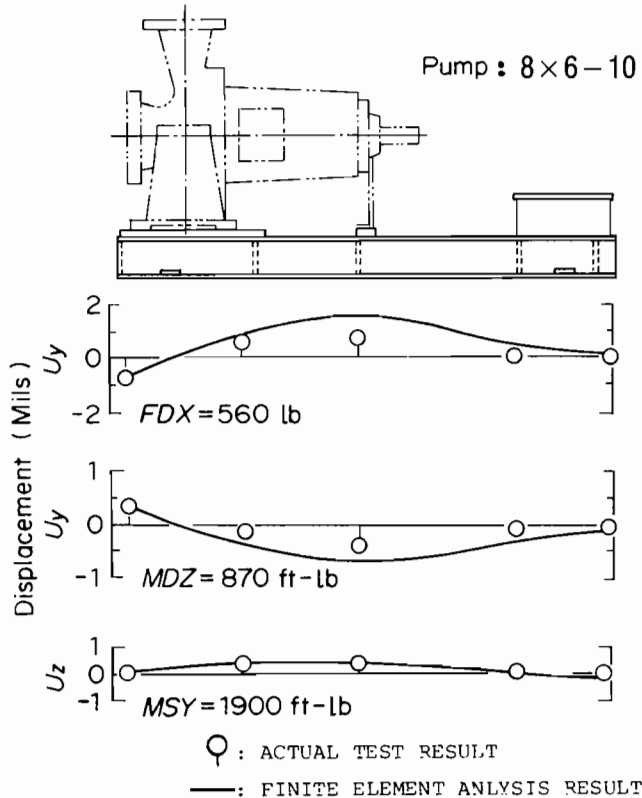


Figure 12. Baseplate Deformation Due to Applied Nozzle Loads. (8 × 6 – 10).

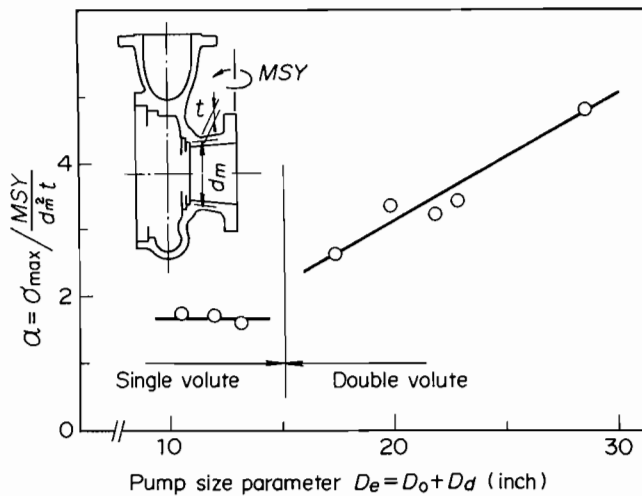


Figure 13. Relationship Between Stress Coefficient and Pump Size Parameter ( $D_e$ ).

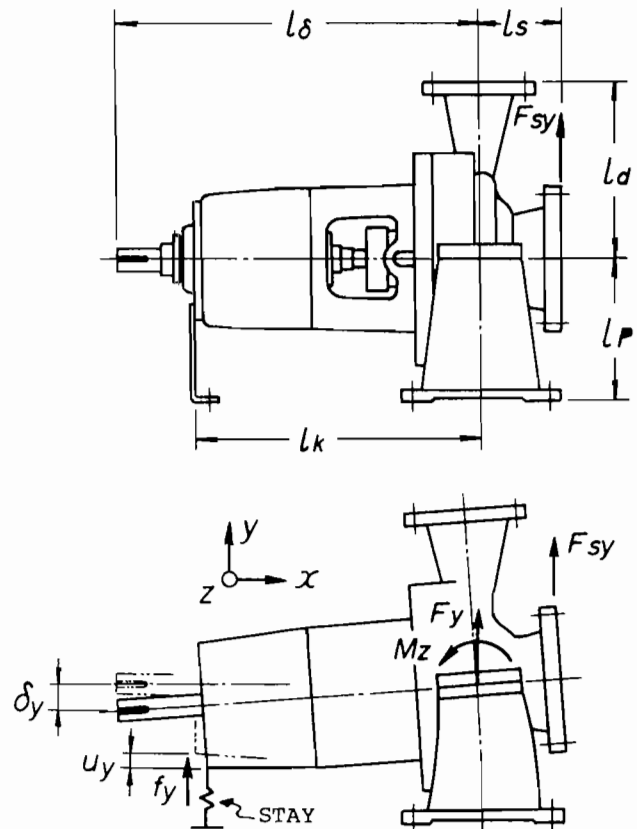


Figure 14. Nomenclature for Shaft End Displacement Analysis.

FORMULAS FOR CALCULATING SHAFT END DISPLACEMENT

The bending stiffness of the pump supports, bearing housing stay and baseplate must be known. These stiffnesses can easily be calculated, because supports, stays and baseplates have simple properties.

The shaft end displacement,  $U_p^*$ , is calculated with the assumption that the pump casing and bearing housing are rigid.

An example is illustrated in Figure 14, when a force,  $F_{sy}$  acts on the suction nozzle. The pedestal acts to support the pump casing with  $F_y$  and  $M_z$  at the pedestal centerline. In addition, the force  $f_y$  acts to support the pump bearing housing from the stay. The following equations are derived from balancing these forces:

$$F_{SY} = F_Y - f_Y \tag{1}$$

$$F_{SY} \times 1_s = M_z + (f_y \times 1_k) \tag{2}$$

The displacement of the stay,  $U_y$ , is calculated as follows:

$$U_y = (F_Y/2K_y) - (M_z \times 1_k/K_n \times 1_p) \tag{3}$$

where

- $F_y$  = Support force at pedestal (Y direction)
- $K_y$  = Support stiffness (Y direction)
- $M_z$  = Support moment at pedestal (about Z axis)
- $K_n$  = Support stiffness to moment (about Z axis)

also

$$f_y = -k_y \times U_y \tag{4}$$

where

- $k_y$  = Stiffness of bearing housing stay (Y direction)
- $U_y$  = Stay displacement (Y direction)
- $f_y$  = Force at stay (Y direction)

When Equations 1, 2, 3, 4 are solved for  $M_z$  and  $F_y$ , the following are obtained:

$$M_z = \frac{F_{SY} \times (1_s + K_y \times (1_s + 1_k)/2K_y)}{1 + \frac{k_y}{2K_y} + \frac{K_y \times 1_k \times 2}{K_n \times 1_p}} \tag{5}$$

$$F_y = (F_{SY} (1_s + 1_k) - M_z)/1_k \tag{6}$$

$$U_p^* = \left( \frac{F_y}{2K_y} \right) - \left( \frac{M_z \times 1_k}{K_n \times 1_p} \right) \tag{7}$$

However, this is not the actual shaft deflection because it was assumed that the pump casing and bearing housing were rigid. Therefore, empirical correction factors were developed by dividing  $U_p^*$  into the actual shaft displacements which were calculated by finite analysis.

$$\text{Shaft end displacement correction factor} = \beta (F_{SY}) = \frac{U_p}{U_p^*} \tag{8}$$

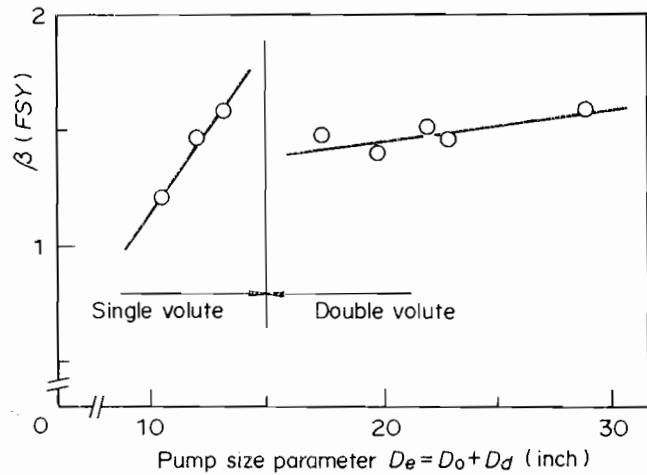


Figure 15. Relationship Between Nondimensional Displacement and Pump Size Parameter ( $D_e$ ).

$\beta(F_{SY})$  corresponds to the deformation of the casing, bearing housing and particular pedestal. Also,  $\beta(F_{SY})$  is proportional to pump size parameter ( $D_e$ ), because the construction of the casing and bearing housing are proportional to  $D_e$ . The relationship for both single volute and double volute pumps is illustrated in Figure 15.

The preceding was an example for  $F_{SY}$  only; however, the same relationship can be developed for all other nozzle loads which cause relatively large shaft end displacement.

Similarly, equations for shaft end displacement caused by deformation of the baseplate can also be obtained. It must be assumed that the main beams of the baseplate receives the pure bending moment. However, shaft deflection due to baseplate deformation is negligible for heavy duty baseplates which are suitably anchored and grouted during installation.

FORMULA APPLICATION

It has been proven that actual test and finite element analysis results generally agree for casing stress and shaft displacement values. This allows the pump manufacturer to calculate casing stress coefficients ( $\alpha$ ) and shaft end displacement correction factors ( $\beta$ ) for various nozzle loads on each size of pump.

These coefficients and correction factors will allow the pump application engineer to use simple formulas for checking the maximum casing stress and the shaft deflection caused by nozzle forces and moments. However, it should be noted that even though these empirical formulas apply to end suction, centerline supported pumps; the values shown for  $\alpha$  (Figure 13) and  $\beta$  (Figure 15) apply to the specific pump model line tested (Ebara Model UCW). These values may differ for other manufacturers with different pump and pump support designs.

CONCLUSION

The behavior of deformation and stress caused by nozzle loads on API 610, end suction pumps has been analyzed in detail. Actual load monitoring experiments and finite element analysis methods were utilized.

The casing stress and shaft end displacement are both proportional to nozzle loads. When several loads are applied simultaneously, the shaft end displacement can be obtained by the arithmetic sum of the displacements due to each individual load. On the other hand, casing stress has no cancelling effects from simultaneous loads because every load generates high stress in a different direction and location. These reactions apply to other API 610, end suction pumps of a similar design.

In addition, the following are more detailed results which only apply to the analyzed pump construction:

- The MSY nozzle load generates a larger casing stress than other nozzle loads.
- As long as the "nominal stress" of the pump-to-pedestal bolts is less than 60 percent of the yield strength, the actual bolt stress is only several percent greater than the initial recommended tightening stress.
- The nozzle loading will not normally cause internal contact at the casing wear rings, throat bushings, seals, etc.
- Shaft end displacement due to nozzle loads is mainly attributed to bending deformation of the pump pedestals, bearing housing stays and baseplate. Casing deformation and bolt elongation have little influence. The most effective methods for increasing allowable nozzle loads are to increase support stiffnesses (support and bearing housing stay) and the number of baseplate anchor bolts.

Formulas for maximum casing stress and shaft end displacement due to nozzle loads were derived. These allow a rapid check for the application engineer, when applying the analyzed pump line.

Based on the results of this study, design changes have been made to ensure that the tested line of pumps meets API 610 Sixth Edition design criteria.

## REFERENCES

1. American Petroleum Institute, "Centrifugal Pumps for General Refinery Services," *API Standard 610, Sixth Edition* (1981).
2. Simon, C.A., "Allowable Pump Piping Loads," *Hydrocarbon Processing*, pp. 98-101 (June 1972).
3. Bussemaker, E.J., "Design Aspects of Baseplates for Oil and Petrochemical Industry Pumps," *Mechanical Engineering C* 45-81, pp. 135-141 (1981).
4. Steiger, J.E., "Horizontal Process Pump Modifications to Comply with API-610 Sixth Edition Forces and Moments," *Proceedings of the First International Pump Symposium*, Turbomachinery Laboratories, Department of Mechanical Engineering, Texas A&M University, College Station, Texas, pp. 47-55 (May 1984).